Treatment of Acid Mine Drainage with Fly Ash: Removal of Major, Minor Elements, SO_4 And Utilization of the Solid Residues for Wastewater Treatment.

W.M. Gitari[1], V.S. Somerset[2], L.F. Petrik[1], D. Key[3], E. Iwuoha[2] and C. Okujeni[4]

[1]Environmental Remediation Group; [2]Sensor Research Laboratory; [3]Department of Chemistry; [4]Department of Earth Sciences; University of the Western Cape, Private Bag X17, Bellville, 7535, South Africa.

KEYWORDS: Fly ash; Acid mine drainage; Co-disposal reaction; Akaline hydrothermal; Zeolites; Sulphates;Wastewater treatment; Metal ions, Scanning electron microscopy.

Introduction

Both acid mine drainage and fly ash from coal burning power generation pose substantial environmental and economic problems for South Africa. The annual national fly ash burden generated by electricity generating companies stands at 27.7Mton [1].Leachates from stockpiled fly ash (FA) are highly siliceous, calcium rich, and extremely alkaline (pH >12). Acid mine drainage (AMD) is highly acidic (pH 2-4), sulphate-rich and frequently carry a high transition metal and heavy metal burden. It is produced when groundwater comes into contact with sulphide minerals that are undergoing oxidation. The extreme pH levels, mineralization, ionic content and toxicity of these wastes are sufficiently environmentally damaging to require expensive storage, remediation and disposal techniques.

Fly ash consists of fine, powdery particles that are predominantly spherical in shape, either solid or hollow. They are considered to be a ferro-alumino silicate made up of glass spheres of very small particle size ranging from 20 to 80 μm with elements Si, Al, Fe, Ca, K and Na being predominant within the matrix [2,3]. The mineralogy of fly ash is greatly influenced by the parent coal from which it was derived. The principal components of bituminous coal fly ash prevalent in South Africa are silica, alumina, iron oxides and calcium oxide with varying amounts of carbon as indicated/measured by the loss on ignition (LOI). Fly ash has a high degree of alkalinity due to the presence of lime fraction. An analysis of Eskom fly ash material has shown that many contaminants are present [4]. Fly ash is normally pumped in slurry form to ash heaps after carbon extraction and hardens to a rock like consistency over time. The wastewater in the disposal slurry as well as rainfall leaches out toxic metals, anions and cations from the ash heaps which pose an environmental hazard.

Several techniques have been developed for the treatment of acid mine drainage which include lime neutralization [5], limestone neutralization [6], biological sulphate removal [7], biological metal removal [8] and ferrite process [9, 10] for heavy metal removal. The principles and methods behind the passive and active treatment of AMD are well researched but alternative liming materials that would decrease the costs of treatment are constantly being sought. Electricity generating companies utilizing pulverized coal are in constant search of better/beneficial fly ash disposal methods.
Several research workers have looked at the efficiency of fly ash to adsorb cations from aqueous solutions and most of them have reported the successful removal of most cations except Hg [11-15].
Several research studies have also been carried out on the application of fly ash for the control of acid generation from sulphidic wastes[16,17] and for amendment of acidic soils [18]. This involves blending the mine spoils and the acidic soils with varying % of fly ash. The fly ash controls the acid generation by the addition of alkalinity to the system and neutralization of the acidity produced. The fly ash also reduces the hydraulic conductivity of the mine spoils.

Recent studies have shown that treatment of acid mine drainage (AMD) with fly ash is possible [19]. Moreover most of the power stations generating the fly ash in South Africa are usually located near the coal mines servicing them hence making the process economically viable. The neutralization capacity of natural AMD with fly ashes from several power stations was investigated and the performance compared with lime and limestone used in the industries for the treatment of acid mine water [20]. The author observed that higher % of fly ash than lime or limestone was required to reach the same pH in the process waters. Another researcher [21] neutralized fly ash with HCL at varying concentration and observed formation of crystals on the spherical surfaces with loss of coatings on some of the spheres. This study tried to relate the neutralization reaction of fly ash with the dissolution of Ca, Mg, and Al from the particles into the solution. In another related study [22] fly ash was titrated with different volume of acid and pH changes monitored as a function of time and the acid volume added, they also equilibrated an acid mine drainage with fly ash and evaluated the metal removal from solution. They observed a pattern whereby the basic metals Ca and Na were released at higher pH and the acidic metals Fe and Cr at lower pH. They further observed that fly ash and fluidised bed ash can be used to treat AMD but their overdose could lead to trace metal accumulation with negative consequences to the environment.
A better understanding of the solution chemistry of the neutralization reaction with respect to element removal and release from fly ash will be important for the fly ash/AMD treatment process. The aim of the current study is to evaluate the neutralization potential of fly ash, establish at what ratios and contact time maximum removal of contaminants is achieved and what mineral phases are precipitating out. This study is employing an overhead stirrer reminiscent of liming type treatment of AMD by limestone or lime in most mining houses to agitate the reaction mixtures.

Despite the many environmental issues associated with coal combustion, it will remain a major source of electrical power generation for many years to come. It has therefore

been necessary to look at methods that can be used to produce or manufacture value-added products from fly ash, as potentially shown by several related studies [23,24,25,26]. In this article attention is given to the possible use of fly ash as a neutralising agent in the treatment of AMD and the synthesis of novel products (e.g. ion exchange adsorbents in the form of zeolites) from the filtrates collected in the co-disposal reaction.

Studies on zeolite synthesis [24,25,27] have shown that zeolites can be obtained by hydrothermal treatment of fly ash. Zeolites have important industrial applications such as in catalysis, sorbents for removal of ions and molecules from wastewaters, radioactive wastes and gases, and as replacements for phosphates in detergents [24,28].

In the results reported in this paper, a co-disposal reaction between FA and AMD was explored to determine whether the two harmful effluents could be co-disposed to form filtrates at a near neutral pH. The co-disposal filtrates were then analysed by XRF spectrometry for quantitative determination of SiO_2 and Al_2O_3. XRF analysis of the co-disposal filtrates was followed by a hydrothermal synthesis process to form zeolites, after which the resulting zeolitic material was characterized.

Experimental procedures

XRF characterization of fly ash samples and co-disposal filtrates

Coal fly ash used in these experiments were obtained from two South African power plants (Matla and Arnot) which combust pulverized coal to generate electricity. The AMD samples used were collected from Navigation colliery and Brugspruit liming plant in Highveld. The Brugspruit AMD samples were seepage from an old abandoned mine and were scooped from the seepage point while Navigation AMD samples consisted of acidic water pumped from underground old mine workings to a collection dam. Results presented in this paper are for reactions between Brugspruit, Navigation AMD and Matla fly ash.

The characteristics of the fly ash samples and co-disposal filtrates used in these experiments are presented in Tables 1.1, and 1.2 below respectively.

Table 1.1: Chemical characteristics of fly ashes used in these experiments – Major elements

Major elements(%)	Arnot fly ash	Matla fly ash		Co-disposal Filtrate
SiO2	53.390 (2.390)	53.771(0.296)		57.03
TiO2	1.342 (0.054)	1.439 (0.110)		1.3
Al2O3	23.402 (1.086)	26.169(2.517)		23.52
Fe2O3	4.721(0.963)	3.402(0.237)		5.7
MnO	0.059 (0.002)	0.047(0.018)		0.16
MgO	2.698(0.045)	2.481(0.579)		2.61
CaO	8.434(0.574)	8.503(1.749)		6.22
Na2O	0.351(0.253)	0.493(0.052)		0.0
K2O	0.493(0.032)	0.863(0.066)		0.59
P2O5	0.348(0.216)	0.608(0.223)		0.24
Cr2O3	0.033(0.009)	0.026(0.006)		0.02
NiO	0.011(0.0007)	0.009		0.02
V2O5	0.0189	0.020		n.a.
ZrO2	0.0516	0.055		n.a.
LOI	2.365 (0.191)	1.327(0.358)		1.99
SiO_2/Al_2O_3	2.28	2.05		2.42

n.a. = not analysed

Table 1.2: Chemical characteristics of fly ashes used in these experiments – Trace elements

Trace elements(ppm)	Arnot fly ash	Matla fly ash
Cu	47.34(6.58)	57.995(9.91)
Mo	5.229	6.562
Ni	93.41(6.49)	58.166(1.12)
Pb	56.35(13.63)	29.077(7.18)
Sr	1463.9(111.8)	2056(205)
Zn	57.33(4.71)	25.357
Zr	488.10(125.7)	536.14(131)
Co	18.25(13.08)	10.35(3.33)
Cr	179.2(1.14)	122.66(27.8)
V	147.4(39)	145.82(32.8)
Ba	928.0(91.9)	1559.2(346)

Before hydrothermal zeolite synthesis was started XRF analysis of the co-disposal filtrates was done for quantitative determination of SiO_2 and Al_2O_3. From this data the $[SiO_2]/[Al_2O_3]$ ratio was determined in order to predict the success of the zeolite synthesis. The XRF results for the co-disposal filtrates are listed in Table 1.1 [29].

The co-disposal filtrate material used for zeolite synthesis was prepared by reacting Arnot FA with Navigation AMD. For the co-disposal filtrate material it was found that the $[SiO_2]/[Al_2O_3]$ ratio is 2.42. When used in hydrothermal zeolite synthesis the co-disposal filtrate material has shown to deliver faujasite, zeolite A and sodalite as zeolitic material [29,30].

When the results obtained for the two different FA sources are compared with that of the co-disposal filtrate metarial, it can be seen that the $[SiO_2]/[Al_2O_3]$ ratios are very comparable. For the Arnot FA the ratio is 2.28 and for the Matla FA it is 2.05. Rayalu [23] reports that if the $[SiO_2]/[Al_2O_3]$ ratio is higher than 1.5, the formation of faujasite as zeolitic material is favoured. It can therefore be predicted that the Arnot and Matla FA, when used in hydrothermal zeolite synthesis, may also deliver a combination of faujasite, zeolte A and sodalite as zeolitic material [30].

The characteristics of the AMD sources used in the experiments are presented in Tables 2 below.

Table 2: Characteristics of AMDs used in these experiments

Parameter	Navigation	Bank	Brugspruit(2)	Brugspruit(1)
pH	2.39	2.46	2.91	1.15
EC(mS/cm)	10.83	10.78	10.02	11.36
Acidity(mg/l $CaCO_3$)	6950(70.7)	7000(70.7)	500(0)	ND
TDS(mg/L)	16765	19410	8975	ND
B	1.37	1.51	2.29	0.66
Na	358.7	399.9	4137.9	96.7
Mg	2661.7	2844.2	388.7	36.5
Al	1068.1	1140.1	60.04	429.5
Si	82.01	87.8	69.7	49.5
K	23.03	19.3	52.6	11.0
Ca	653.3	1012.3	842.1	493.2
Mn	226.3	242.3	31.6	79.2
Fe	5599.9	6115.9	250.8	6338.5
Fe2+	3725.1	2886.3	153.1	ND
Fe3+	1451.9	3344.6	126.1	ND
Ni	6.95	7.96	2.35	2.43
Co	4.3	4.57	1.15	1.35
Zn	48.99	17.7	9.52	13.5
Sr	7.69	8.39	1.05	1.86
Mo	0.04	0.044	0.036	ND
Ba	0.209	0.189	0.148	0.022
SO_4^{2-}	11888.1	14949.7	6155.0	ND
Cl^-	729.3	265.9	720	ND
NO^{3-}	163.2	41.6	BDL	ND

Brugspruit (1)-winter samples, Brugspruit (2)-summer samples, ND-not determined,
BDL-Below detection limits

Raw AMD samples were filtered by using 0.45μm cellulose nitrate membrane to remove suspended particles and diluted with MQ water to EC<1.5mS/cm and then stabilized with HNO_3 for elemental analysis. Samples for anion/cation analysis were filtered by using 0.45 μm cellulose nitrate membrane and kept at 4^oC until analysis. A 24 hour co-disposal experiments were designed to develop neutralization curves that would indicate buffer characteristics/regions and show the contact time required for the attainment of minimum EC values in the process waters. The batch neutralization experiments were conducted by stirring a mixture of fly ash and AMD which was pre-

determined to give a specific fly ash ratio (AMD: FA). The AMD was stirred for 30 minutes for equilibration before the fly ash was added. An overhead stirrer was used for all the experiments. The progress of the reaction was monitored by measuring the pH and EC with a Hanna HI 991301 portable pH/EC/TDS/Temperature meter. Elemental analysis of the water samples was done by ICP-MS (ELAN 6000). The accuracy of the analysis was monitored by analysis of NIST water standards. Fe^{2+}/Fe^{3+} analysis was done by the colorimetric method using 2,2-bipyridal as the complexing reagent. SO_4^{2-} analysis was done turbidimetrically by a portable datalogging spectrophotometer (Hach DR/2010) and ion chromatography.
Chemical characteristics of the fly ash samples was ascertained by X-ray fluorescence spectroscopy (XRF) by fusing with lithium metaborate. The co-disposal solids collected after reacting fly ash with AMD for 24 hours were analysed by PANalytical X-ray diffractometer (XRD) using Cu *Kα* radiation generated at 20 mA and 40 KV. Specimens were step scanned as random powder mounts from 5 to 85^{o} 2θ integrated at 0.1^{o} 2θ per second. X-ray diffraction analysis can detect crystalline phases present at 5 % mass, this method is important in detecting changes in the initial mineralogical changes brought by reaction with AMD. Powder samples of the co-disposal solids were also observed under a scanning electron microscope (SEM) equipped with an energy dispersive X-ray analysis system (EDXA).

Zeolite Synthesis

In the zeolite synthesis method the co-disposal filtrates were fused with sodium hydroxide (NaOH) in a 1:1.2 ratio at 600 ºC for about 1 – 2 hours. The milled fused product was then mixed thoroughly with distilled water and the slurry was subjected to aging for 8 hours. After aging the slurry was subjected to crystallisation at 100 ºC for 24 hours. The solid product was recovered by filtration and washed thoroughly with deionised water until the filtrate had a pH of 10 to 11. The product was then dried at a temperature of 70 ºC [23].

Results and discussion

Chemical characteristics of materials used in this experiments

Matla and Arnot fly ash

The three major phases Al_2O_3, Fe_2O_3 and SiO_2 do not vary to a great extent (Table1.1). Matla fly ash has higher Al_2O_3 content while Arnot fly ash shows higher Fe_2O_3 content. The American Society for Testing and Materials [31] uses these three major phases to classify fly ashes based on source coal. From the analysis (SiO_2 +Al_2O_3+Fe_2O_3≥ 70%) the South African fly ashes are class F which are either derived from anthracitic or bituminous coals [3]. The CaO content shows slight variation with Matla fly ash showing a slightly higher value. The total CaO content detected by XRF does not distinguish the free lime from that trapped within the glass matrix. The free CaO content is important because it will dissolve into solution at a faster rate than will the calcium contained

within the glass matrix and has implications for the pH of the resulting process water on contact with AMD. Among the minor elements both fly ashes shows high concentrations of Sr, Ba, Cr, Zr and Ni (Table 1.2). Trace elements of Mo are also present. These concentrations are within the concentration ranges reported for fly ashes [32], which indicates that they are higher than values generally found in coals and soils indicating that the combustion process tends to enrich the fly ash with the minor elements.

Brugspruit and Navigation AMD

The pH values of the samples ranged from 1.15 for Brugspruit (1) to 2.92 for Brugspruit (2) indicating strongly acidic waters (Table 2). The pH of mine water can be driven towards acidic or alkaline mode depending on the relative abundance and extent of weathering of pyrite and calcite neutralization. pH values in the acidic mode imply a deficiency of calcareous minerals and absence of carbonate buffering in these AMD samples. All the samples exhibit high electrical conductivity (10.02-11.36) mS/cm). Azzie [33] observed electrical conductivities ranging from (4.0-13.7) mS/cm in some South African coal mine waters, the SO_4^{2-} correlated positively with the EC measurements for most of the acidic coal mine waters investigated. The SO_4^{2-} recorded in these samples ranged from (6155.0 –11888.1) mg/l and was the dominant anion. Major cations included Na, Ca, Mg, Al, Mn and Fe. Dissolution of silicate minerals such as feldspar, kaolinite, chlorite accounts for most or all of the dissolved K, Na, Mg, Al and Ca [34].
Brugspruit (2) samples collected in summer had low iron concentration compared to Brugspruit (1) samples collected in winter but had high concentrations of Na, Mg and Ca.

The ferrous iron in these samples represented half or greater proportion of the total iron (Table 2). In most samples of coal mine drainage, an abundance of dissolved ferrous iron (Fe^{2+}) indicates that the chemical reactions are at an intermediate stage in the series of reactions where pyrite is being directly oxidized by the Fe^{3+} (Equation 1) [35].

$$FeS_2(s) + 14\ Fe^{3+} + 8\ H_2O = 15Fe^{2+} + 2\ SO_4^{2-} + 16\ H^+ \quad \text{.....(1)}$$

Neutralization reactions

Figure 1 shows the pH trends for the neutralization reactions between Brugspruit (1) AMD and Matla fly ash (samples collected in winter) and Figure 2 shows the same pH trends for Brugspruit (2) AMD samples collected in summer and Matla fly ash. The reactions between Navigation AMD, Bank AMD and Matla fly ash are included for comparison (Figure 3 and 4).

Similar pH trends were observed for the AMD: FA ratios investigated for the three AMD samples except Brugspruit (2) samples. All the three (Brugspruit (1), Navigation and Bank) AMD samples investigated show a strong buffering capacity at pH (5.5 -6.0) at the highest AMD: FA (3:1) ratio investigated. This buffering region is associated with

oxidation and hydrolysis of Fe^{2+} which releases H^+ ions and delays rise in pH [36]. Fe^{2+} accounted for half of the total iron in the AMD samples investigated (Table 2). Only Bank AMD exhibited a buffer region at pH 4.0 for AMD: FA ratio of 3:1 and 1.5:1. Bank AMD samples had the highest Fe^{3+} concentration than the other AMD samples (Table 2). The buffering in this region is due to hydrolysis of dissolved Fe^{3+} which releases H^+ and delays rise in pH [37]. A slow increase in pH is observed after the buffer region (pH 4.0) Al hydrolysis with subsequent release of H^+ ions occurs at this pH (4.3-5.5)[37]. The lower concentration of Al compared to Fe^{3+}/Fe^{2+} explains the weaker buffering observed. At intermediate ratios (2.5:1, 1.5:1) two buffer regions were observed at pH 6.0 and pH (9.0-10.0),(Table 3 and 4). A fourth buffer region was observed at pH (11.0-12.0) (Figs 1 and 4). At longer contact times all the AMD: FA ratios investigated were observed to equilibrate at pH >11 (Fig 1).

Neutralization curves for Brugspruit (2) AMD samples deviated from the trend observed for the three other samples (Brugspruit (1), Navigation and Bank. (Fig 2). This AMD sample had very low buffering capacity. Most of the AMD: FA ratios (Figs 2, 3, 4) used were high as compared to reactions with Brugspruit (1), Bank and Navigation but breakthrough to alkaline pH was observed within five minutes of contact (Fig 2) as opposed to Brugspruit (1), Bank and Navigation where breakthrough to alkaline pH occured after (90-240 minutes) of contact. The Brugspruit (2) AMD samples had very low concentration of Fe^{3+}/Fe^{2+}, Al and Mn (Table 2) than the other three samples and these could account for the lack of the buffer regions

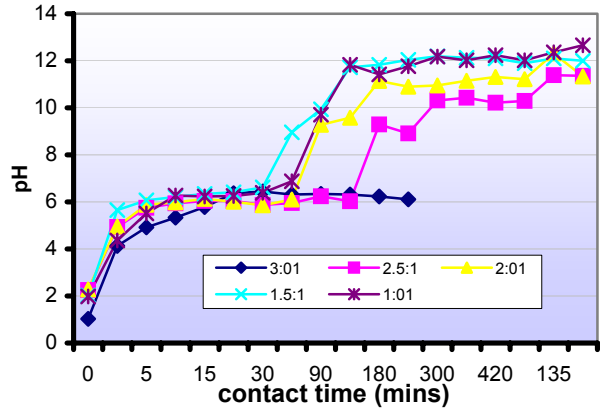

Figure 1: Variation of pH with contact time (mins) for various AMD: FA ratios for Brugspruit (1) AMD and Matla fly ash reactions

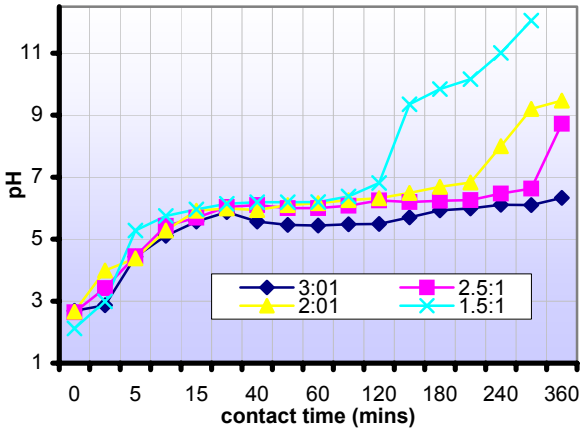

Figure 3: Variation of pH with contact time (mins) for various AMD: FA ratios for Navigation AMD and Matla fly ash reactions

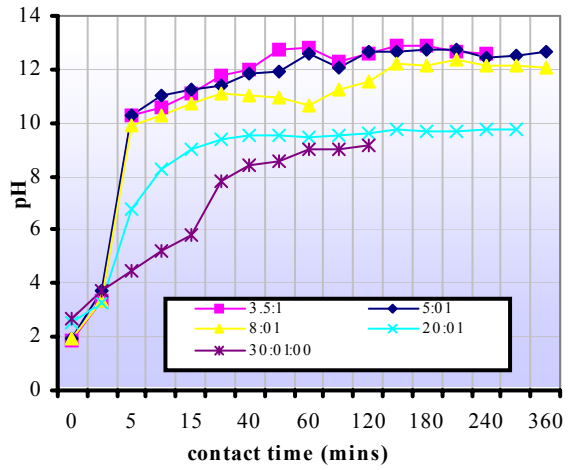

Figure 2: Variation of pH with contact time (mins) for various AMD:FA ratios for Brugspruit (2) AMD and Matla fly ash react

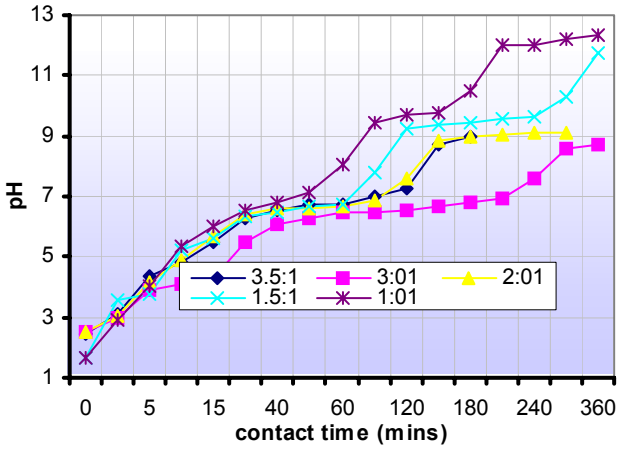

Figure 4: Variation of pH with contact time (mins) for various AMD:FA ratios for Bank AMD and Matla fly ash.

Metal removal trends as a function of AMD: FA ratios in the final process waters

Figure 5 below shows the change in pH for final process water and Figures 6-10 shows the removal trends of metals in the final process waters for the AMD: FA ratios investigated for Brugspruit (2) AMD and Matla fly ash. Figure 11 shows the removal trends of SO_4^{2-}, Cl^- in final process waters. Figure 12 shows the change in pH for final process water and Figures 13-17 shows the removal trends of metals in the final process waters for the AMD: FA ratios investigated for Navigation AMD and Matla fly ash while Figure 18 shows the trends for the removal of $SO_4^{2-}$and Cl^-.

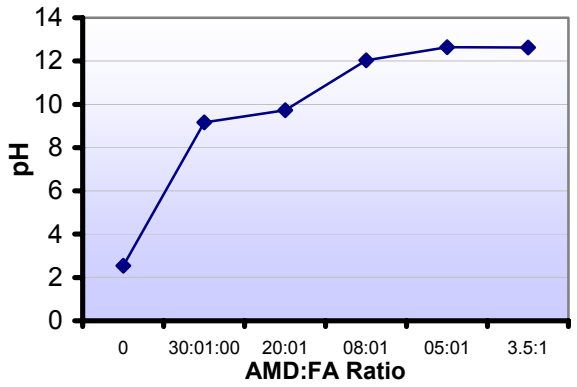

Figure 5: Change in pH of final process water with AMD: FA ratio for Brugspruit (2) and Matla fly ash

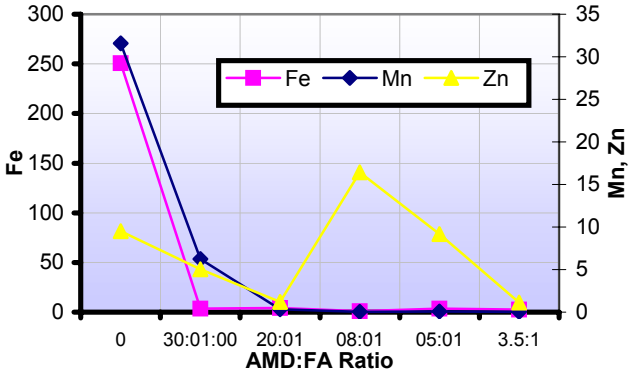

Figure 7: Concentration of Fe, Mn, Zn (mg/l) in final process waters with AMD:FA ratio for Brugspruit (2) and Matla fly ash

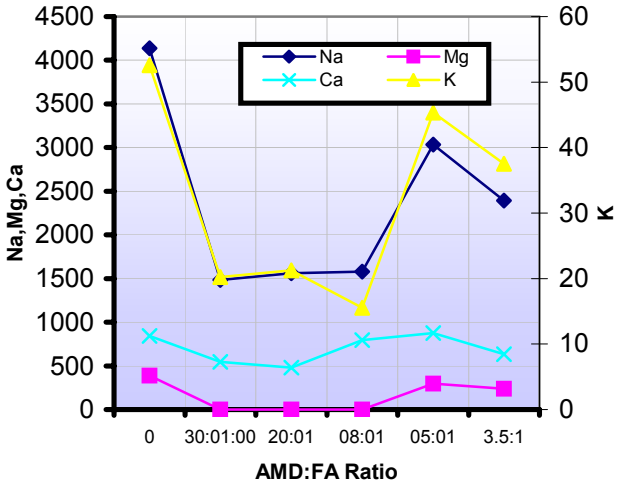

Figure 6: Concentration of Ca, Na, Mg, K (mg/l) in final process waters with AMD:FA ratio for Brugspruit (2) and Matla fly ash

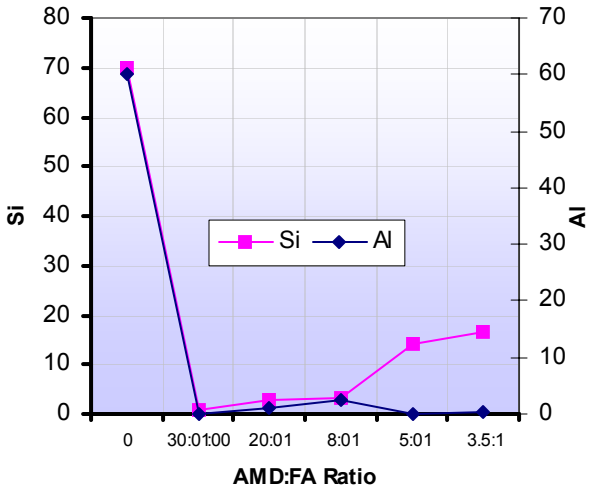

Figure 8: Concentration of Si, Al (mg/l) in final process waters with AMD:FA ratio for Brugspruit (2) and Matla Fly ash.

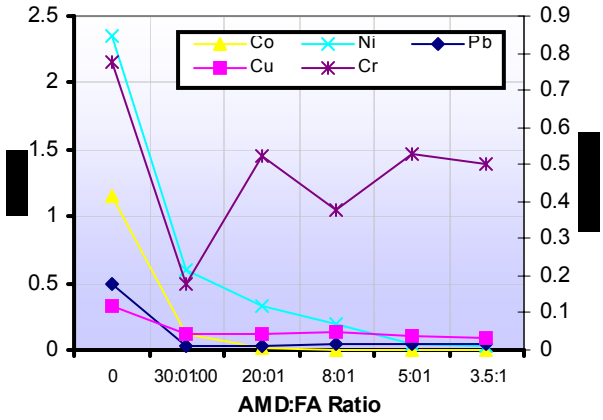

Figure 9: Concentration of Co, Ni, Pb, Cu, Cr (mg/l) in final process waters with AMD:FA ratio for Brugspruit (2) and Matla fly ash

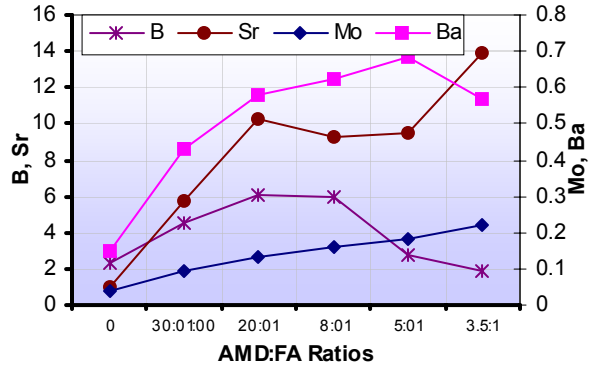

Figure 10: Concentration of B, Sr, Mo, Ba (mg/l) in final process waters with AMD:FA ratio for Brugspruit (2) and Matla fly ash

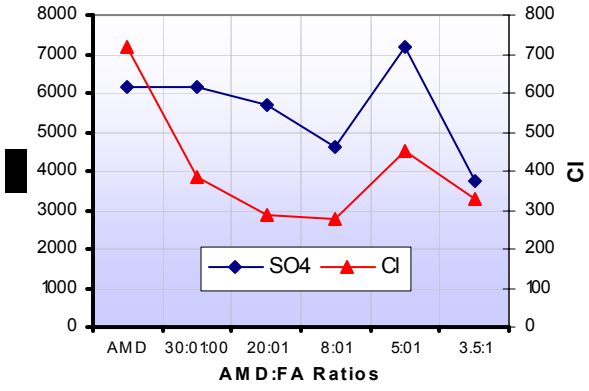

Figure 11: Concentration of SO4, Cl (mg/l) in final process waters with AMD:FA ratio for Brugspruit (2) and Matla fly ash

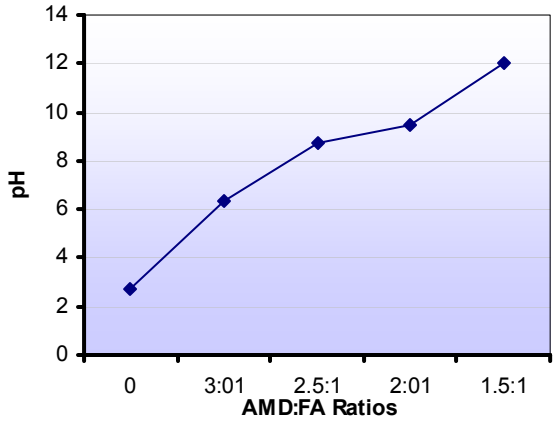

Figure 12: Change in pH of final process water with AMD: FA ratio for Navigation and Matla fly ash

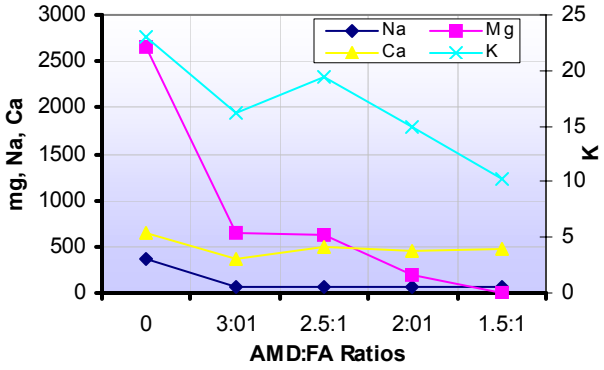

Figure 13: Concentration of Na, K, Mg, Ca (mg/l) in final process waters with AMD:FA ratio for Navigation and Matla fly ash

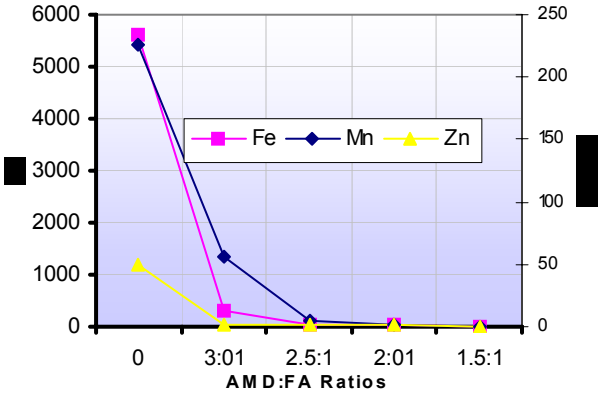

Figure 14: Concentration of Fe, Mn, Zn (mg/l) in final process waters with AMD:FA ratio for Navigation and Matla fly ash

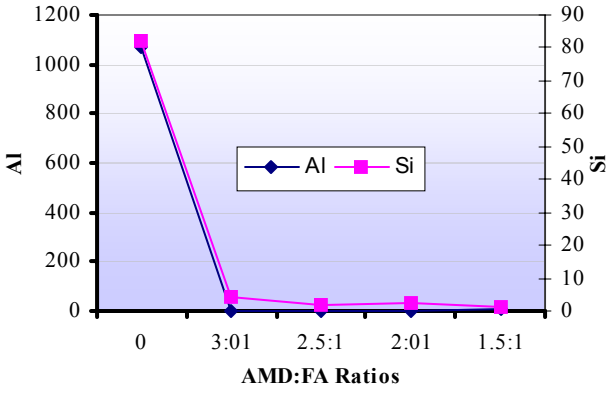

Figure 15: Concentration of Al, Si (mg/l) in final process waters with AMD: FA ratio for Navigation and Matla fly ash

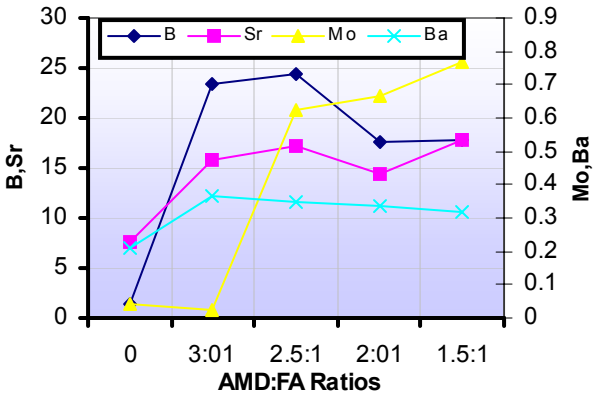

Figure 17: Concentration of B, Sr, Mo, Ba (mg/l) in final process waters with AMD:FA ratio for Navigation and Matla fly ash

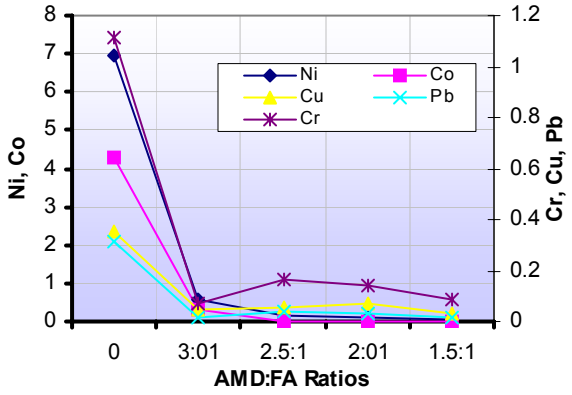

Figure 16: Concentration of Ni, Co, Cu, Pb, Cr (mg/l) in final process waters with AMD: FA ratio for Navigation and Matla fly ash

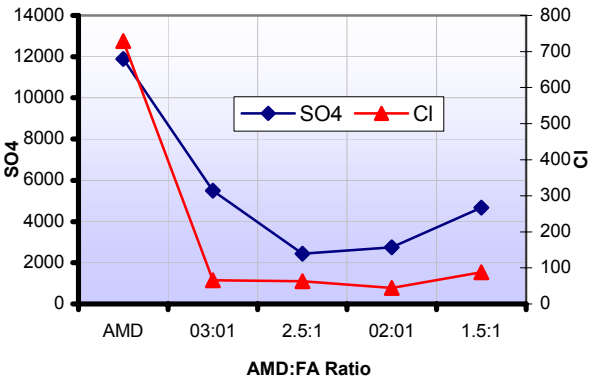

Figure 18: Concentration of SO_4^{2-}, Cl^- (mg/l) in final process waters with AMD: FA ratio for Navigation and Matla fly ash

pH in final process waters

All the AMD: FA ratios investigated for Brugspruit(2) attained a pH>9.0(Fig 5) while for Navigation the final pH was quite distinct for each ratio(Fig 11). Despite the higher AMD: FA ratios used for Brugspruit(2) reactions, breakthrough to alkaline pH was attained within (5-60) minutes of contact (Fig 2). The lack of buffering capacity for Brugspruit (2) was attributed to the low concentration of Fe^{3+}, Fe^{2+} Al^{3+}, Mn [37].

Major and trace elements in final process waters: Brugspruit (2) AMD reactions

The concentrations of Na, K, Ca and Mg exhibit a similar trend as the AMD: FA ratio decreases. At intermediate ratios 30:1, 20:1 8:1 minimum concentrations were

observed. At lower ratios 5:1, 3.5:1(Fig 6) an increase in solution was observed. Jenke [38] observed that treatment of acidic waters with alkaline reagents leaves Ca, K, Na in the process waters. Major elements Fe, Mn, Si, Al are significantly reduced in all the ratios investigated. Zn and Al are noted to increase at the intermediate ratio of 8:1 while Si shows a steady increase with increasing fly ash in the mixture (decrease in AMD: FA ratio). At the pH (12.0-12.5)(Fig 5) for ratios 8:1, 5:1, the formation of hydroxide complexes is likely to increase the solubility of Zn and Al. Dissolution of the silica in fly ash and high solubility of Si at this pH could account for the increase in concentration. Minor elements Co, Ni, Cu, Pb are observed to decrease significantly for all AMD: FA ratios investigated. Cr decreases to a minimum (0.8 mg/l) at 30:1 ratio followed by an increase which stabilizes at values of between 0.36-0.5 mg/l as the fly ash is increased in the reaction mixture. Recent laboratory studies indicate that Cr is present in fly ash as Cr^{3+} [39] and at pH 9.0 observed for ratio 30:1 (Fig 5) Cr will precipitate out as $Cr(OH)_3$ but as pH increases to >11 (Figs 5 and 9) the $Cr(OH)_4^-$ dominates. Ba, Mo and Sr are observed to increase steadily with increasing fly ash in the reaction mixture (Fig 10). High concentrations of Ba and Sr were observed in the Matla fly ash (Table 2) suggesting dissolution of soluble salts of these elements from fly ash accounts for the high concentrations observed in the process waters. The trends for Mo also suggests dissolution of its soluble salt from fly ash particles. Eary (1990) [32] observes that the rates at which minor elements are leached from unweathered fossil fuel wastes are dependent on the abundances, accessibility to solution and dissolution kinetics. B increases steadily to a maximum at 2:1 ratio followed by a decrease with increasing fly ash in the mixture (Fig 10). Hullet [40] observes that B occurs as surface oxide precipitates or incorporated in the glassy matrix of fly ash and its concentration will initially be limited by dissolution rates of the surface precipitates and glassy particles and by adsorption on the precipitates that form. At the high pH 12.0-12.5 (Fig 5) lower values of B were observed. Hollis [41] observed that B concentrations are likely to be lowest in alkaline leachates that are actively precipitating $CaCO_{3\,(s)}$.

The SO_4^{2-} and Cl^- concentrations were observed to decrease steadily with increasing fly ash in the mixture. The deviations at the ratio of 5:1 was due to desorption of SO_4^{2-} and Cl^- at the high pH (Fig 5) when the solution was left in contact with the reacted fly ash before filtration. Rose and Crawford [43] reported that SO_4^{2-} rich AMD when treated with alkaline reagents and left in contact with the iron oxyhydroxides precipitates at alkaline pH (= 7.0) desorption of 30 - 40 % of the oxalate-soluble SO_4^{2-} occurs. The desorption is due to competition between OH^- and SO_4^{2-} for adsorption sites at the high pH.

Navigation AMD reactions

Treatment of Navigation AMD with Matla fly ash leaves Ca, and K as the major cations in solution. Ca and Na decrease is observed for 3:1 ratio but thereafter remains constant with increasing fly ash in the reaction mixture. K concentrations decreases steadily with decreasing AMD: FA ratios (Fig 14). Mg is observed to decrease steadily with increasing fly ash in the mixture. Britton [42] observed that at pH >10.49 Mg precipitates out and should be out of solution at pH 11. However a significant quantity of Mg is lost from solution at a lower pH suggesting other mechanisms could be

responsible for the loss of Mg. The ratio 1.5:1 had a final pH of 12.0 corresponding to the lowest levels of Mg (1.50 mg/l) observed in the process waters (Fig 12). Fe, Mn, Zn showed (Fig 14) considerable removal at ratio 3:1 but complete removal is observed with decreasing AMD: FA ratio, at ratio 1.5:1 lowest values for the three elements were observed (Fe=4.7mg/l, Mn=0.133mg/l, Zn=0.736mg/l). Jenke [38] observes that at pH 3.0 of Fe3+, pH 6.0-8.0 for Fe^{2+}, pH 8.41-9.0 for Mn and pH 6.0-6.5 for Zn^{2+} a significant portion of the initial concentration should be precipitated out of solution. The final pH for the process waters for the ratios investigated varied from 6.0-12.0 (Fig 12) suggesting that precipitation could be the main mechanism for removal of these elements. Minor elements Ni, Co, Pb are increasingly removed in process waters with increasing fly ash in the mixture. This corresponds to the increasing pH of the final process waters (Fig 12). An observation of the pH of precipitation of these elements (pH= 6.66 for Ni^{3+}, pH=6.81 for Co^{3+}, pH=6.0 for Pb^{2+}) from Britton [42] are within the pHs observed in these experiments (Fig 12). At intermediate ratios 2.5:1, 1.5:1 Cu^{2+} and Cr^{2+} were observed to increase marginally then decreasing at ratio 1:1. Formation of hydroxide complexes at pH>10 increases the solubility of Cu^{2+} and could be responsible for the increased concentration. Domination of $Cr(OH)_4^-$ at pH>10 increases the solubility of Cr^{3+} and accounts for the increased concentration [39]. An increase is observed for B and Sr at ratios 3:1 and 1.5:1(Fig 17) followed by a marginal increase at ratio 1.5:1. Formation of borates (BO_3^{3-}) at high pH >10 and their incorporation into calcite and aluminium hydroxides could account for the decreasing concentration at the lower AMD: FA ratios [32, 43]. Ba is observed to increase at the ratio 3:1 followed by a marginal decrease for the rest of the ratios (Fig 17). Mo concentration in final solution increased as the fly ash increased in the reaction mixture indicating possible lack of solubility control [44]. The solution concentration of Mo in this process was influenced by the AMD: FA ratio.

Significant SO4 removal was observed at the higher AMD: FA ratios of 3:1, 2.5:1 with 50 % of the total SO4 being removed at the contact time investigated. SO4 present in AMD can sorb to iron oxyhydroxides and precipitate to form a variety of minerals such as gypsum, jarosite and amorphous sulfate–bearing iron oxyhydroxide phases [45]. Marginal increase of SO4 was observed as the fly ash increased in the mixture (Fig 18). Rose and Ghazi [46] observes that SO4 partitions upon sites of variable bond energy ranging from strong bidentate oxygen bridges to surfaces where weak electrostatic attractions predominate, its this portion attached to the iron oxyhydroxide surfaces by electrostatic attractions that is labile at high pH and accounts for the marginal increase as the pH increases in the final process waters. Cl^- closely followed the same trend.

XRD results

XRD diffractograms of the unreacted fly ash revealed mullite, quartz and alumino-silicate as the main phases. The AMD reacted fly ash revealed gypsum as the only new phase formed. XRD is often not sensitive to the development of small quantities of secondary mineral phases or alternatively the phases were amorphous to X-rays.

Use of zeolitic material in metal ion removal experiments

A set of laboratory scale experiments was performed in which the synthesized zeolitic material was reacted with acid mine drainage (AMD) in different doses (g/100 ml). The metal ion removal experiments were carried out with aliquots of 100 ml of AMD to which zeolite powder doses of 0.5, 1, 1.5 and 2 g/100 ml were added [29].

This was done to observe if any reduction in the concentrations of selected metal ion species could be observed after the AMD was treated with the synthesized zeolitic material. These experiments were performed on the working hypothesis that the use of a product containing a high proportion of zeolites (e.g. FAU, SOD, zeolite A), with a fraction of alkaline fly ash particles, it could raise the pH and induce a favourable environment for ion exchange [25].

In the experiments performed, the AMD was also treated with a commercial faujasite zeolite (ComFAU), in order to compare the metal ion removal results with that of the co-disposal filtrate zeolite sample (CodFAU) prepared from the co-disposal filtrate material. The results obtained for the metal ion removal experiments are shown in Figures 19 to 20 [47].

In Figure 19 it is observed that the Ni concentrations gradually decreased as the ComFAU zeolite dosage was increased and a lower final concentration was obtained. With the addition of CodFAU zeolite a relatively bigger decrease in the Ni concentrations of the AMD was obtained than with the use of the commercial product.

Figure 19. Ni concentrations of AMD after treatment with commercial zeolite (ComZ) and FA zeolite (FAZ1) respectively.

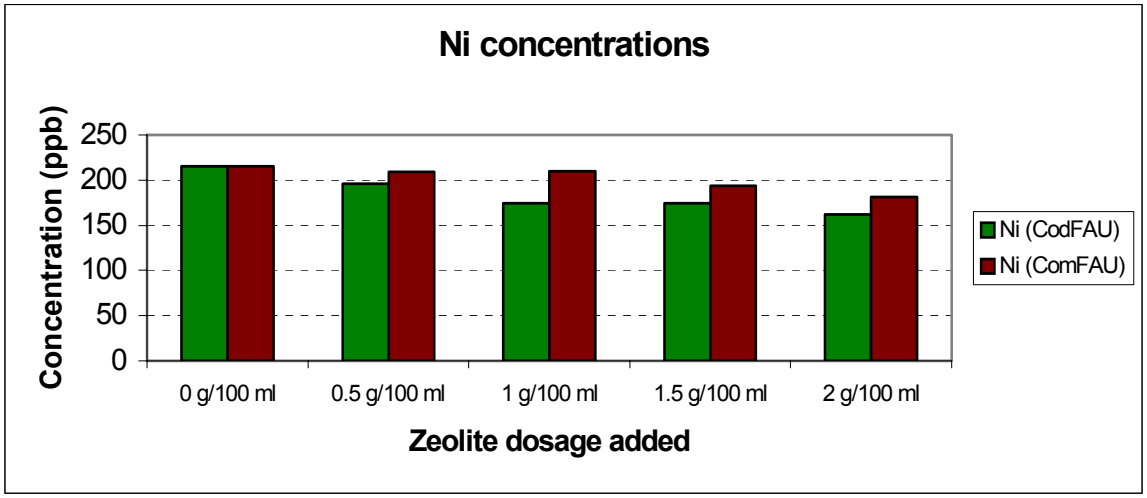

In Figure 20 it is observed that in the treatment of the AMD with CodFAU an initial increase was observed in the concentration after which it gradually decreased (with increasing zeolite dosage) to a lower concentration than in the initial AMD. With the use of ComFAU the results showed that the Zn concentrations remains relatively unchanged as the zeolite dosage was increased.

The best metal ion removal results were obtained for the removal of lead from the AMD with CodFAU, as shown in Figure 21. A much lower Pb concentration than the initial one detected was obtained for the highest CodFAU zeolite dosage added. For the use of the ComFAU zeolite, increases in the Pb concentration was observed, with the final Pb concentration at the highest zeolite dosage added, being higher than the initial Pb concentration [47].

Figure 20. Zn concentrations of AMD after treatment with commercial zeolite (ComZ) and FA zeolite (FAZ1) respectively.

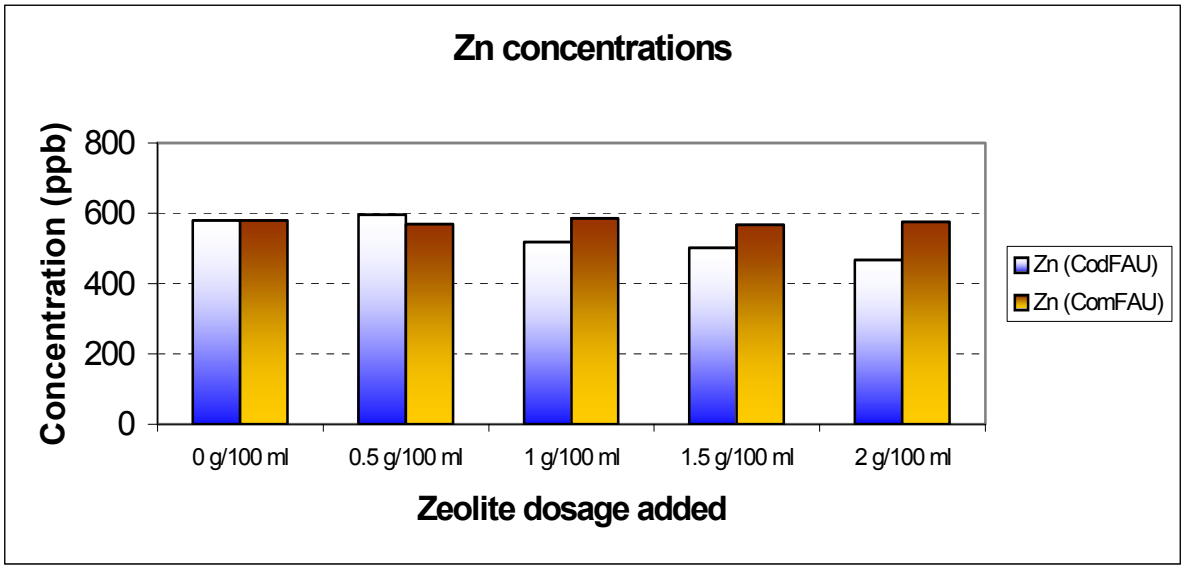

Figure 21. Pb concentrations of AMD after treatment with commercial zeolite (ComZ) and FA zeolite (FAZ1) respectively.

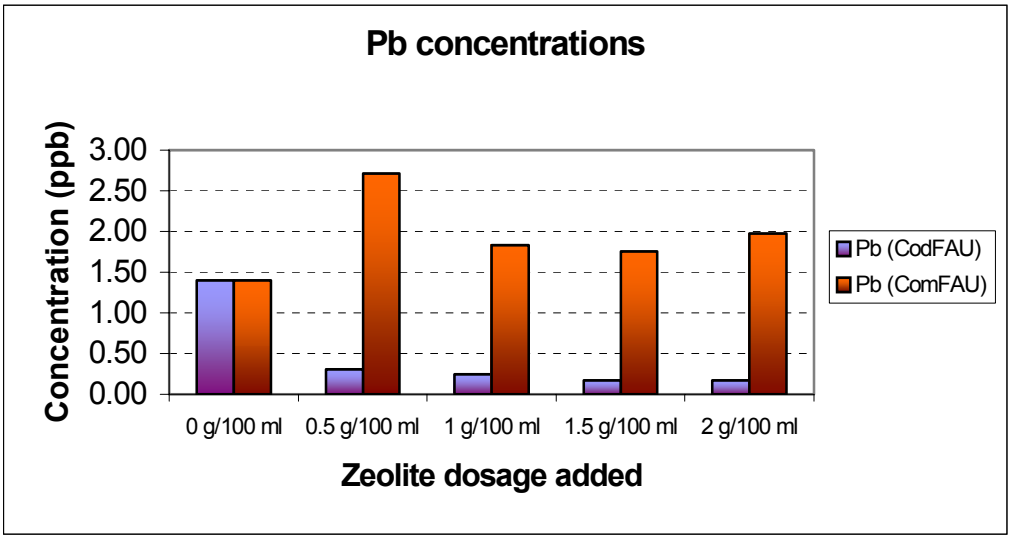

Conclusions

In absence of buffering regions associated with Fe^{2+}, Fe^{3+} and Al^{3+}, dissolution and precipitation are the main processes controlling the concentrations of major and minor elements in the process water. High AMD: FA ratios and short contact times are required for complete removal of the elements from solution. Desorption of SO_4^{2-} was observed to be greatest in this system when the co-disposal solids are in contact with the treated water at high pH. In presence of buffering by Fe^{2+}, Fe^{3+} and Al^{3+} the removal of major and minor elements is slower due to the slow increase in pH and oxidation of Fe^{2+}. Lower AMD: FA ratios and longer contact times (90-360 minutes) would be required for complete elements removal.
SO_4^{2-} removal is observed to be greatest for system exhibiting strong buffering with 79.1 % (Fig 18) of the total SO_4^{2-} being removed as opposed to 49.3 % (Fig 11) for the system exhibiting weak buffering.

A co-disposal reaction between fly ash and acid mine drainage can be used to form co-disposal filtrates at a near neutral pH, providing a source of Al and Si for zeolite hydrothermal synthesis. A [SiO2]/[Al2O3] ratio higher than 2 obtained for the co-disposal filtrates proves to be successful in converting the filtrates into faujasite, sodalite A and zeolite A zeolitic material. The [SiO2]/[Al2O3] ratio is higher in the co-disposal filtrate material, than in the Arnot and Matla FA sources itself. However, with the [SiO2]/[Al2O3] ratio higher than 2 in both the FA sources, it can be safely predicted that they can also successfully be converted to faujasite zeolitic material, through hydrothermal zeolite synthesis.

Furthermore, the use of the synthesized zeolitic material in metal ion removal experiments have shown that in the treatment of the AMD, the CodFAU zeolite was more effective in removing Ni, Zn and Pb ions from the AMD, compared to the use of the commercial zeolite, ComFAU.

ACKNOWLDEGEMENTS

The authors wish to express their gratitude to the Water Research Commission (WRC), Coaltech 2020 Consortium, and the National Research Foundation (NRF) for funding and financial support to perform this study. We would also like to express our gratitude to the CSIR and ESKOM, for their assistance in the collection of samples. Special thanks to the Chemistry Department of the University of the Western Cape for the assistance provided during this study.

REFERENCES

[1] Krüger E. Japie. South African fly ash: a cement extender. A publication by the South African coal ash association (2003.

[2] Adriano D.C, A.L. Page, A.A. Elseewi, A.C. Chang, and I. Straughan. Utilization and Disposal of Fly Ash and Other Coal Residues in Terrestial Ecosystems: A Review*. J. Environ. Qual.,* 1980, Vol. 9, No. 3,

[3] Mattigod S.V., Dhanpat Rai., L.E. Eary, and C.C. Ainsworth. Geochemical Factors Controlling the Mobilization of Inorganic Constituents from Fossil Fuel Combustion Residues: Review of the Major Elements. *J. Environ. Qual.* 1990,19:188-201.

[4] Campbell A. Chemical, physical and mineralogical properties associated with the hardening of some South African fly ashes. *MSc thesis*, 1998. University of Cape Town, RSA.

[5] Geldenhuys, A.J., J.P. Maree., M. de Beer. and P. Hlabella. An integrated limestone/lime processes for partial sulphate removal. *The journal of The South African Institute of Mining and Metallurgy.* 2003.

[6] Maree J.P. and G.J Van Tonder. Limes tone neutralization of Iron (II) rich acid water.*WISA biennial conference*, Suncity, South Africa, 28th May to 1st June 2000.

[7] Maree J.P., H. Greben and S. Mnqanqeni., Simultaneous removal of sulphate and sulphide with the biosure process from coal acid mine drainage. *WISA 2000 Biennual conference*, Suncity, South Africa.

[8] Cheong, Y.W., Min, J.S., Kwon, K.S. Metal removal efficiencies of substrates for treating acid mine drainage of the Dalsung mine, *South Korea. J. Geochem. Exlor*. 1998. 64, 147-152.

[9] Wang W, Xu Z and Finch. Fundamental study of an ambient temperature ferrite process in the treatment of acid mine drainage. *Environ Sci. Technol* 1996. 30, 2604-2608.

[10] Y.Tamaura ., T. Katsura., S. Rojarayanont., T. Yoshida and H.Abe. Ferrite process; Heavy metal ions treatment system. *Water science technology*. 1991, Vol 23, Kyoto, pp1893-1900.

[11] Babel Sandhya, Tonni Agustiono Kurniawan. Low-cost adsorbents for heavy metals uptake from contaminated water: A Review. *Journal of hazardous materials* 2003. B97, 219-243.

[12] Panday K.K, Gur Prasad and V.N. Singh Copper (II) removal from aqueous solutions by fly ash. *Water Research*. 1985. Vol 19, No. 7, pp. 869-873.

[13] Apak Resat, Esma Tutem, Mehmet Hugul and Julide Hizal. Heavy metal cation retention by unconventional sorbents (red muds and fly ashes). *Water Research*. 1998. Vol. 32, No2, pp. 430-440.

[14] Hequet V., Ricou P, I. Lecuyer and P. Le Cloirec. Removal of Cu^{2+} and Zn^{2+} in aqueous solutions by sorption onto fly ash and fly ash mixtures. *International ash utilization symposium*, Center for applied energy research, University of Kentucky, 1999. paper no 42.

[15] Ricou P, V. Hequet, I. Lecuyer and P. Le Cloirec. Influence of operating conditions on Heavy metal cation removal by fly ash in aqueous solutions. *International ash utilization symposium*, Center for applied energy research, University of Kentucky, 1999. paper no 42.

[16] Xenidis Anthimos, Evangelia Mylona, Ioannis Paspaliaris. Potential use of lignite fly ash for the control of acid generation from sulphidic wastes. *Waste Management* 2002. 22, 631-641.

[17] Seoane S and Leiros M.C. Acidification-Neutralization processes in a Lignite mine spoil amended with fly ash or limestone. *J. Environ. Qual*. 2001. Vol. 30, July-August.

[18] Phung H.T, L. J. Lund, A. L. Page, and G.R. Bradford. Trace elements in fly ash and their release in water and treated soils. *J. Environ. Qual*., 1979,Vol. 8, No. 2,

[19] WRC/Coaltech 2020 project K5/1242, Simultaneous water recovery and utilisation of two harmful effluents, fly ash leachate and acid mine drainage, for the production of high capacity inorganic ion exchange material useful for water beneficiation, 2003.

[20] Klink. M. The potential use of South African coal fly ash as a neutralization treatment option for acid mine drainage. *MSc Thesis*. 2004. University Of The Western Cape.

[21] Hodgson L, Dan Dyer, and D.A. Brown. Neutralization and dissolution of High-Calcium fly ash. *J. Environmental Quality*., Vol. 11, no. 1, 1982.

[22] Karapanagioti H.K and Atalay A.S. Laboratory evaluation of ash materials as acid-disturbed land amendments. *Global Nest: J.* 2001,*Vol* 3, No 1, pp 11-21.

[23] Rayalu, S.; Meshram, S.U.; Hasan, M.Z. Journal of Hazardous Materials, 2000**,** B77, pp. 123-131.

[24] Querol, X.; Plana, F.; Alastuey, A.; López-Soler, A. Fuel*,* 1997, 76 (8), pp. 793-799.

[25] Querol, X.; Moreno, N.; Ayora, C.; Pereira, C.F.; Janssen-Jurkovicová, M. Environmental Science & Technology, 2001a, 25 (17), pp. 3526-3534.

[26] Querol, X.; Umaña, J.C.; Plana, F.; Alastuey, A.; López-Soler, A.; Medinaceli, A.; Valero, A.; Domingo, M.J.; Garcia-Rojo, E. Fuel, 2001b**,** 80, pp. 857 – 865.

[27] Hollman, G.G., Steenbruggen, G. & Janssen-Jurkovicová, M. Fuel, 1999, 78, p. 1225-1230.

[28] Singh, D.N. & Kolay, P.K. Progress in Energy & Combustion Science, 2002, 28, pp. 267-299.

[29] Somerset, V.S. Unpublished M.Sc. Thesis. (2003) University of the Western Cape, Bellville, RSA.

[30] Somerset, V.S., Petrik, L.F., White, R.A., Klink, M.J., Key, D. & Iwuoha, E. Talanta, 2004, 64, pp. 109-114.

[31] American Society for Testing and Materials. Standard specification for fly ash and raw or calcined natural pozzolan for use as a mineral admixture in Portland cement concrete. 1988. C618-88. ASTM, Philadelphia, PA.

[32] Eary L.E., Mattigod S.V., Dhanpat Rai. and C.C. Ainsworth. Geochemical Factors Controlling the Mobilization of Inorganic Constituents from Fossil Fuel Combustion Residues: Review of the Minor Elements. *J. Environ. Qual.* 1990, 19:188-201.

[33] Azzie, B. A-M. Coal mine waters in South Africa: Their geochemistry, quality and classification. *PhD Thesis*, 2002. University of Cape Town, SA.

[34] Crouse, H.L. and A.W. Rose. Natural beneficiation of acid mine drainage by interaction with stream water and stream sediment. In: 6th Symposium on Coal Mine Drainage Research, National Coal Association/Bituminous Coal Research, Inc., 1976, pp. 237-269.

[35] Stumm,W. and J.J. Morgan. Aquatic chemistry. Wiley Interscience, 1981, p.470.

[36] Stumm, W and Lee, G.F. Oxygenation of ferrous iron. Industrial and Engineering Chemistry. 1961 53(2), 143-146.

[37] Uhlmann W, H. Buttcher, O. Totsche, and C.E.W. Steinberg. Buffering of Acidic Mine Lakes: The Relevance of Surface Exchange and Solid bound Sulphate. Mine Water and Environment. 2004, 23: 20-27.

[38] Jenke R.D and Gordon K. P. Chemical changes in concentrated, Acidic, Metal-bearing waste waters when treated with Lime. *Environ. Sci. Technol*, 1983, Vol, 17, No 4.

[39] Rai, D., R.W. Szelmecka. Aqueous behaviour of chromium in fly ash. J. environmental quality. 1990, 19 (3).

[40] Hullet, L.D., and A.J. Weinberger. Some etching studies of the microstructure and composition of large aluminosilicate particles in fly ash from coal burning power plants. *Environ. Sci. Technol*. 1980, 14: 965-970.

[41] Hollis, J.F., R. Keren, and M.Gal. Boron release and sorption by fly ash as affected by pH and particle size. *J. Environ. Qual*. 1988, 7: 181-184.

[42] Britton, H.T.S. Hydrogen ions, fourth edition. Chapman and Hall, London 1956.

[43] Kitano Yasushi, Minoru Okumura and Masatoshi Idogaki. Coprecipitation of Borate-boron with calcium carbonate. *Geochemical Journal*, 1978, Vol. 12, pp 183-189.

[44] Reardon E.J., C.A. Czank, C.J. Warren, R. Dayal, and H. M. Johnson. Determining controls on element concentrations in fly ash leachate. *Waste Management and Research*. 1995, 13, 435-450.

[45] Bigham J.M., Schwertmann., U, Taina, S.J., Winland, R.L., Wolf, M. *Geochim. Cosmochim. Acta* 1996, 60, 2111-2121.

[46] Rose Seth and A. Mohamed Ghazi. Release of Sorbed sulfate from iron oxyhydroxides precipitated from acid mine drainage associated with coal mining. *Environ. Sci. Technol*, 1997, 31, 2136-2140.

[47] Somerset, V.S., Petrik, L.F., Iwuoha, E.I. Journal of Environmental Science & Health – Part A, 2005, A40 (8), (in press).